IEEE Photonics Journal
An IEEE Photonics Society Publication

Open Access

Dynamic Ratiometric Imaging of Cytosolic Free Ca^{2+} in Skeletal Muscle Cells Using 340/385-nm Light-Emitting Diode Illuminators

Volume 10, Number 6, December 2018

Manoop Chenchiliyan
Dana Adler Portal
Ruchira Chakraborty
Tal Shahar Ben-Gal
Assaf Deutsch
Eliahu Pewzner
Asher Shainberg
Hamootal Duadi
Dror Fixler

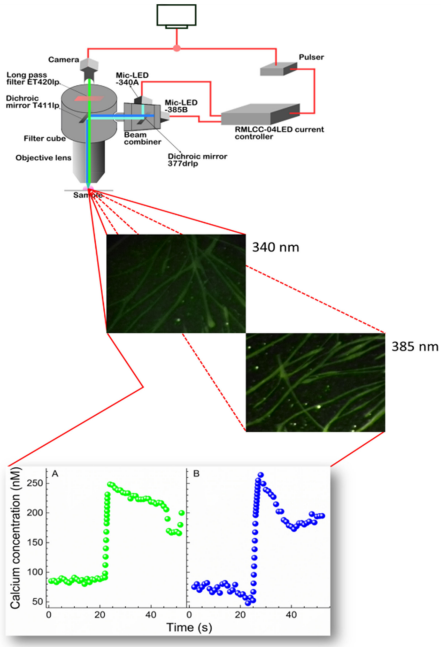

DOI: 10.1109/JPHOT.2018.2882503
1943-0655

Dynamic Ratiometric Imaging of Cytosolic Free Ca^{2+} in Skeletal Muscle Cells Using 340/385-nm Light-Emitting Diode Illuminators

Manoop Chenchiliyan,[1] Dana Adler Portal,[2] Ruchira Chakraborty,[1] Tal Shahar Ben-Gal,[1] Assaf Deutsch,[3] Eliahu Pewzner,[3] Asher Shainberg,[2] Hamootal Duadi,[1] and Dror Fixler [1]

[1]Faculty of Engineering and the Institute of Nanotechnology and Advanced Materials, Bar-Ilan University, Ramat Gan 5290002, Israel
[2]Faculty of Life Sciences, Bar Ilan University, Ramat Gan 5290002, Israel
[3]Prizmatix Ltd., Givat-Shmuel 5410102, Israel

DOI:10.1109/JPHOT.2018.2882503

Manuscript received October 26, 2018; revised November 15, 2018; accepted November 16, 2018. Date of publication November 20, 2018; date of current version December 6, 2018. Corresponding author: D. Fixler (e-mail: Dror.Fixler@biu.ac.il).

Abstract: Calcium-sensitive fluorescent indicators fall broadly into two categories, ratiometric (dual-wavelength) or single-wavelength indicators based on their response to a calcium elevation. Ratiometric indicators shift either their excitation or their emission wavelengths in response to calcium, allowing the concentration of intracellular calcium to be determined from the ratio of fluorescence emission or excitation at distinct wavelengths. Fura-2 is one of the most common ratiometric fluorescent Ca^{2+} indicators, which has an emission maximum at 510 nm whereas its excitation maximum changes from 380 to 340 nm in response to calcium binding. Historically, a combination of arc lamp and monochromators has been used as the light source for Fura-2 ratiomatric fluorescence microscopy. In recent years, different combinations of LEDs such as 350/380 nm or 360/380 nm have been used to excite Fura-2. To precisely match the Fura-2 excitation, in this study, we built a new fast switchable 340/385-nm LED excitation light source (Prizmatix Ltd., Israel). The newly constructed light source has been exploited in Fura-2 ratiometric calcium imaging of skeletal muscle cells. The spontaneously elicited Ca^{2+} transients in the cells were recorded with high temporal resolution. The light source utilized for the demonstrated instrumentation in this report optimally matches the excitation wavelengths of either calcium-free or bound states of Fura-2. The high-intensity stability and fast switching of the 340/385-nm LED illuminators indicate their potential as a preferred light source for Fura-2 ratiometric calcium imaging over the existing light sources.

Index Terms: Ratio-metric imaging, fluorescence, microscopy, Fura-2, LED, calcium imaging, rat myotubes.

1. Introduction

The intracellular concentration of free ionized calcium (Ca^{2+}) plays a key role in triggering a range of cellular events including the contractile activity of muscle cells, neurotransmitter release, and oocyte fertilization [1]–[3]. The critical evaluation of the role of calcium as an intracellular messenger,

therefore, requires a quantitative measurement of cytosolic free Ca^{2+} concentrations. Due to the diversity of cellular Ca^{2+} signaling in different types of cells [4], [5], there is no gold standard with which one can monitor Ca^{2+} changes in all situations [6]–[12]. However, Ca^{2+} sensitive fluorescent indicator and imaging is considered as the most flexible and widely used technique for measuring cellular Ca^{2+} responses.

Calcium-sensitive fluorescent indicators fall broadly into two categories: ratio-metric (dual-wavelength) or single-wavelength indicators based on their response to the calcium elevation. Although the single-wavelength indicators, such as Fluo-4, provides high dynamic range, they cannot compensate for the Ca^{2+} signal changes caused by indicator concentration, photo-bleaching, extrusion, or compartmentalization [13]. At the same time, the ratio signal obtained using a dual-wavelength indicator is independent of the dye concentration, illumination intensity, and optical path length allowing the concentration of intracellular calcium to be determined independently of these artifacts.

Ratio-metric indicators shift either their excitation (for example Fura-2) or their emission (for example Indo-1) wavelengths in response to calcium, allowing the concentration of intracellular calcium to be determined from the ratio of fluorescence emission or excitation at distinct wavelengths [14], [15]. The dual-excitation ratio-metric indicator Fura-2, and dual-emission ratio-metric indicator Indo-1 are the most widely used ratio-metric fluorescents indicators in calcium imaging techniques [16]. Both of these indicators have been extensively used to study cell calcium metabolism, diffusion of Ca^{2+} in the cytosol, intracellular propagations of Ca^{2+}, excitation-contraction coupling in muscle cells and more [17]–[21].

In comparison with Indo-1; Fura-2 is less susceptible to photo-bleaching, and has a relatively higher dynamic range between Ca^{2+} bound and free states [13], [22]. Fura-2 has an emission maximum at 510 nm whereas upon binding Ca^{2+} its excitation maximum undergoes a shift from 380 nm to 340 nm, see Section 2.3 [16]. Historically, a combination of arc lamp and monochromators have been used for the sequential excitation of Fura-2 at 340 and 380 nm in ratio-metric cytosolic Ca^{2+} imaging. In recent years, light emitting diodes (LEDs) have been employed as a preferred excitation light source for Fura-2. Compared with arc lamps, a LED excitation source has much higher stability, faster-switching speed and feasibility of precisely controlling the output intensity by adjusting the LED driver current. However, until recently, due to the commercial unavailability of shorter wavelength LEDs, the excitation sources were restricted to a combination of either 350/380 nm or 360/380 LEDs, which do not exactly match the required excitation wavelengths of Fura-2. To precisely match Fura-2 excitation, in this study we built a new fast switchable 340/385 nm LED excitation light source. The newly constructed light source has been exploited in Fura-2 ratio-metric calcium imaging of skeletal muscle cells. The spontaneously elicited Ca^{2+} transients in the cells were recorded with a high temporal resolution.

2. Materials and Methods

2.1 Cell Culture

The experiments were carried out by the guidelines of the Animal Care and Use Committee of Bar-Ilan University, and the Guide for the Care and Use of Laboratory Animals published by the US National Institute of Health. Sprague Dawley rat pups (1–2 days of age, from Harlan, Israel) were killed by decapitation. Muscle cultures were prepared as described elsewhere [23], [24]. Briefly, skeletal muscle from the thigh was removed under sterile conditions and washed three times in PBS to remove excess blood. Muscles were minced into small fragments and gently agitated in PBS containing 0.05% trypsin, which resulted in the release of single cells. The suspension was then centrifuged for 5 min at 400 $\times$ g at room temperature. The supernatant was discarded, and cells were re-suspended in Dulbecco's Modified Eagle Medium (DMEM) containing 25 mM glucose and supplemented with 10% heat-inactivated horse serum and 2% chick embryo extract. The cell suspension was diluted in the same medium to 1.0×10^6 cells/ml, and 1.5 ml of cells were then plated in 35 mm collagen/gelatin-coated plastic culture dishes. Cultures were incubated in

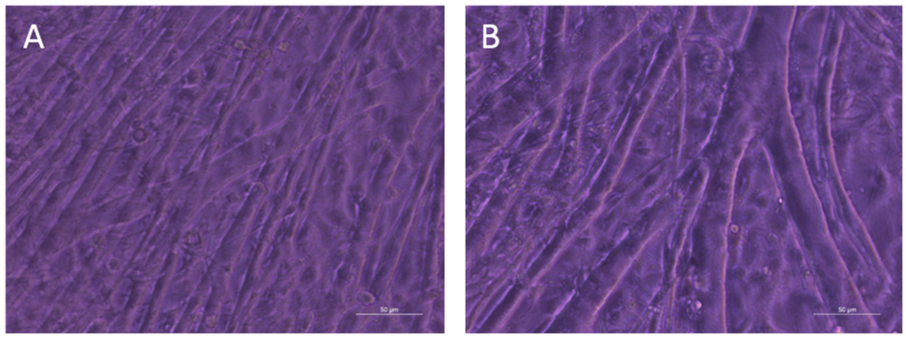

Fig. 1. Images of the fused myotubes captured at two different locations of the 5 day old skeletal muscle cells recorded using an upright microscope respectively with a 10 × N.A 0.4 (A) and 20 × N.A 0.3 (B) objective. The scale bar is presented at the bottom right.

a humidified atmosphere of air with 5% CO_2 at 37 °C. Fused myotubes form within 3–7 days of plating, see Fig. 1.

2.2 The 340/385 nm LED Excitation Light Source

The light source used for the measurements comprised of the Mic-LED-340A collimated LED at about 340 nm, and Mic-LED-385B collimated LED at about 385 nm (Prizmatix Ltd., Israel). The two collimated LEDs are combined by a Beam Combiner OptiBlock (Prizmatix Ltd., Israel) equipped with a dichroic mirror 377drlp (Chroma, Vermont, USA). The two LEDs are connected to the RMLCC-04 current controller. The current controller enables continuous or pulsed operation of the LEDs. The ratio-metric transistor-transistor logic (TTL) input of RMLCC-04 provides an alternating pulsation of the LEDs and synchronization of these light pulses with the camera. The Pulser (Prizmatix Ltd., Israel) was used to create TTL pulse trains for the ratio-metric imaging.

2.3 Characterization of 340/385 nm LED Excitation Light Source

The emission spectra of the combined 340/385 nm illumination LED system were measured at 700 mA and 500 mA current, respectively, using a commercially available UV-VIS spectrometer (EPP2000, StellarNet, Inc., Florida, USA) with a spectral resolution of 0.5 nm. The normalized emission spectra are presented in Fig. 2. The emission maxima of each LEDs were respectively found at 343.63 nm (FWHM: 12.41 nm) and 383.80 nm (FWHM: 13.60 nm).

2.4 Intracellular Ca^{2+} Measurements

The spontaneously triggered calcium signals in rat myotubes were measured using a Fura-2 based ratio-metric fluorescence microscopy imaging. Prior to the Ca^{2+} measurements the cells were loaded with 10 μM of Fura-2 AM (F1201, ThermoFisher, Massachusetts, USA) and 2 μM of pluronic acid (F-127, ThermoFisher, Massachusetts, USA) for 45-60 minutes in the dark at ambient temperature to complete de-esterification of Fura-2 AM in phosphate buffered saline containing calcium and magnesium, and 20 mM glucose (pH 7.4). After de-esterification of Fura-2 AM, the cells were rinsed three times using the buffer solution before imaging. The 35 mm petri dishes containing the cells were imaged with a 10 x N.A 0.4 objective (Olympus UPlanFL N, Tokyo, Japan) mounted on an upright widefield epifluorescence microscope (Olympus BX51, Tokyo, Japan). The combined 340/385 nm excitation light was coupled to the epifluorescence port of the microscope. The fluorescence microscope filter cube was equipped with T411lp dichroic and ET420lp emission filter (Chroma, Vermont, USA). General set-up of the imaging system is schematically illustrated in panel A of Fig. 3. A simulation of the new ratio-metric Ca^{2+} imaging system can be performed online in a dual LED fluorescence spectra viewer developed by Prizmatix Ltd., Israel at https://bit.ly/2wyhLwv.

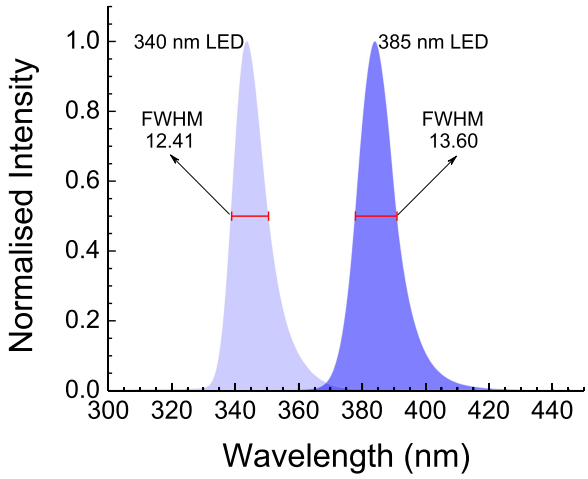

Fig. 2. Normalized emission spectra of 340/385 nm LEDs. The full width at half maximum (FWHM) of each LED is presented in nm.

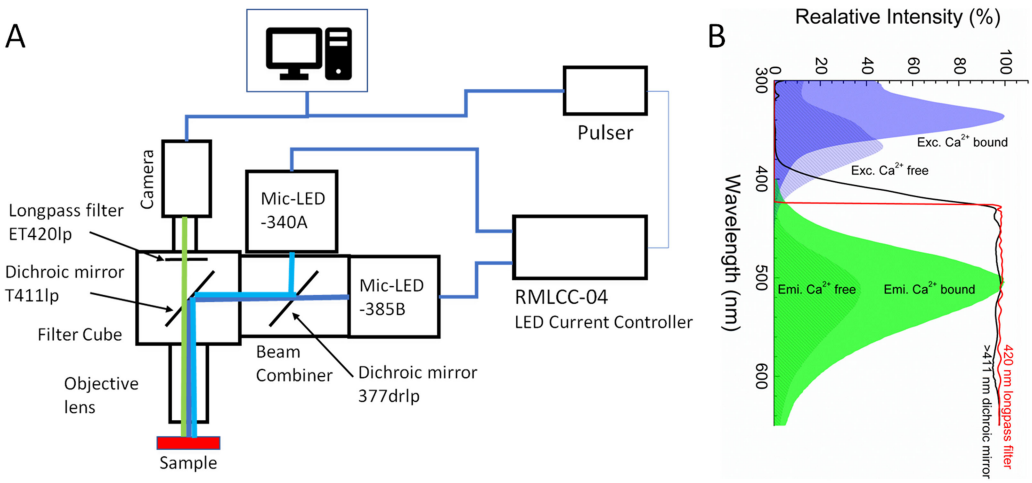

Fig. 3. (A): schematic illustration of the ratio-metric fluorescence microscopy imaging set-up using 340/385 nm LEDs. The beam path of 340 nm, 385 nm LEDs and fluorescence from the cells are respectively indicated by turquoise, blue and green colored lines. (B): the excitation spectra of Fura-2 in a solution containing Ca^{2+} (maximum at 340 nm, blue shaded area) and Ca^{2+} free solution (maximum at 380 nm, blue patterned area). The emission spectra of the Fura-2 is presented in green, which has a maximum at 510 nm regardless of the Ca^{2+} content in the solution. The black and red curves respectively represent the spectral window of the T411lp nm dichroic mirror and the ET420lp nm emission filter. See text for further details.

This viewer allows the user to simulate the excitation and emission spectra of the Fura-2 either in Ca^{2+} free or bound state by inputting the optics used in the actual experiments. The simulation input panel is illustrated in Fig. 4.

To achieve the ratio imaging, the samples were consecutively excited by 340 nm and 385 nm LEDs. The excitation intensities at the specimen plane were 0.46 mW/mm^2 and 0.82 mW/mm^2 respectively for 340 and 385 nm LEDs. The pulse trains from the LEDs are obtained by Pulser, a programmable TTL pulse train generator (Prizmatix Ltd., Israel), which is also used to synchronously trigger the camera with the LED pulses. The exposure time of each LED was 0.8 s at a rate of 10 Hz. The resulting fluorescence emission from the samples was recorded above 420 nm by a complementary metal oxide semiconductor (CMOS) camera (PL-B741, PixeLink, Ottawa, Canada)

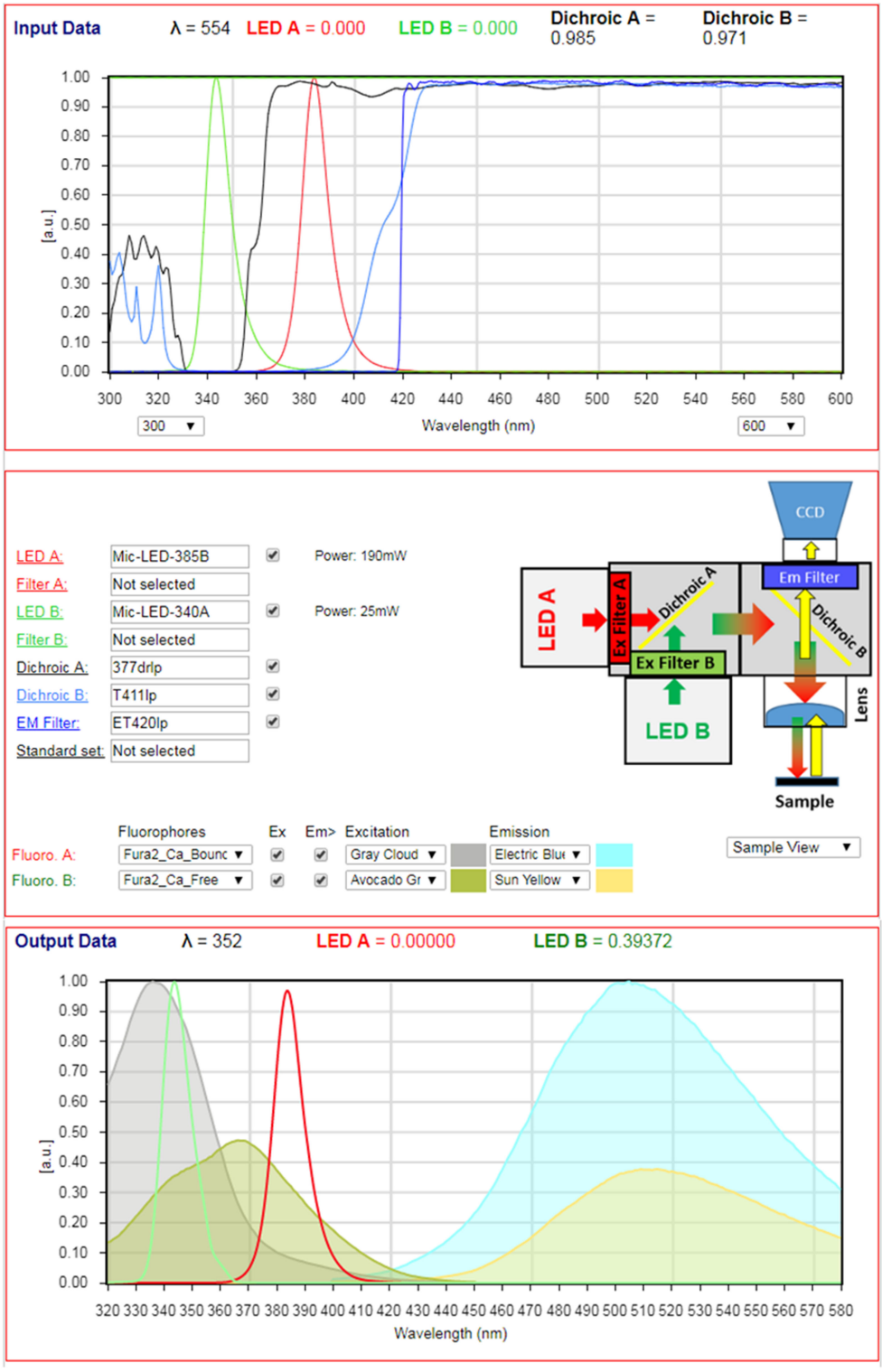

Fig. 4. The input panel of the LED Spectra Viewer: The graph on top shows the simulation input data according to selected LEDs, filters and dichroic mirrors (left side below the graph). The sketch of the simulated system is presented at the right side. The fluorophore to be excited by the LEDs are at the bottom. The output panel shows the LED spectra, fluorophore excitation, and emission spectra. The presented output spectra of LEDs and the fluorophore emission spectra are collected through the selected input filters and dichroic mirrors.

using the PixeLink Capture OEM (PixeLink, Ottawa, Canada) image software. The video images were captured for 100 s in every measurement. All cells spontaneously contracting within the viewing field were recorded and analyzed. The intracellular Ca^{2+} changes were accessed using the measured fluorescence ratio, R [16], [25].

2.5 Video Image Processing

The videos reflecting the free intracellular Ca^{2+} changes upon the spontaneous contraction of the cells were first loaded into a MATLAB script [26]. The script extracts the frames of the video corresponding to 340, and 385 nm LED illumination through the entire duration of the video. The intensity values obtained from each frame is corrected for the background fluorescence level and then the ratio, R, is acquired.

The intracellular free Ca^{2+} concentration was calculated from the fluorescence ratio, R, using the following equation presented in [16],

$$\left[Ca^{2+}\right] = \beta K_d \left(\frac{R - R_{\min}}{R_{\max} - R}\right) \tag{1}$$

where R is the experimental fluorescence ratio of the myotubes under investigation. $R_{\min}$ and $R_{\max}$, respectively the minimum and maximum fluorescence ratio in the absence and saturation levels of Ca^{2+}. β, is the ratio of fluorescence between the absence and saturating levels of Ca^{2+} upon 385 nm illumination. k_d, is the dissociation constant of the binding of Fura-2 with Ca^{2+} (224 nm). The values for β, $R_{\min}$, and $R_{\max}$ are taken from the Ca^{2+} calibration measurements, see the following section.

3. Results

3.1 Calibration of Fura-2

Calibration of fluorescent Ca^{2+} indicators is a prerequisite for accurate Ca^{2+} measurements. It provides the experimental values for β, $R_{\min}$, and $R_{\max}$ so that the intracellular free Ca^{2+} concentration can be evaluated from the fluorescence intensity ratio, R, obtained from the sample of interest. The preparation of Fura-2 calibration solution can be found elsewhere [13], [27]. The cell-impermeant Fura-2 (F1200, ThermoFisher, Massachusetts, USA) dissolved in solutions of various calcium concentrations. The excitation and emission spectra of the cell-impermeant Fura-2 in the absence and saturating levels of Ca^{2+} is presented in panel B of Fig. 3. A similar concentration of Fura-2 as in the intracellular Ca^{2+} measurement was used in the calibration measurements. As expected, while an increase in the fluorescent intensity upon 340 nm excitation as the Ca^{2+} concentration rises, at 385 nm, the opposite occurred, see panel A of Fig. 5. The calculated fluorescence intensity ratio, R, from the measured fluorescence intensities is presented in panel B of Fig. 5. The fluorescence intensity ratio, R, ensures linearly measuring intracellular Ca^{2+} level between $\sim$33 nm to 665 μM.

The following values, 5.23, 0.66 and 7.41 are found from panel B of Fig. 5 respectively for β, $R_{\min}$, and $R_{\max}$.

3.2 Ca^{2+} Resting Level

It has been previously reported that the resting Ca^{2+} levels in rat myotubes loaded with Fura-2 are independent of the cell contraction [28]. Therefore, to determine the resting cytosolic Ca^{2+} concentration, a 5-day old myotube is studied, which is neither spontaneously nor stimulatingly contracting. The petri dish containing the indicator stained 5-day old cells illuminated with the 340 and 385 nm LEDs at different locations of the cells. The representative fluorescence images obtained from the myotubes is presented in Fig. 6. The intensity values from the images measured upon 340/385 nm LED illumination extracted and corrected for the background fluorescence levels. The calculated fluorescence ratio, R, is converted to the cytosolic Ca^{2+} concentration using the Eq. (1). The average resting Ca^{2+} levels in the myotubes are 88 $\pm$ 3 nm.

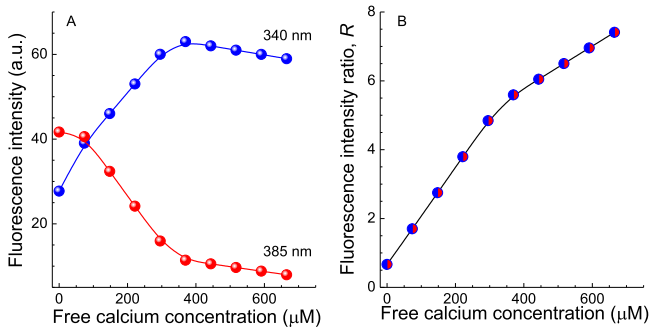

Fig. 5. Fluorescence intensity of 10 μM Fura-2 excited at 340 nm (blue spheres) and 385 nm (red spheres) in solutions of various calcium concentrations (A). The relationship between the ratio of fluorescence intensities of Fura-2 excited at 340 nm and 385 nm and free Ca^{2+} concentrations (B). The fluorescence ratio is calculated using the values presented in panel A.

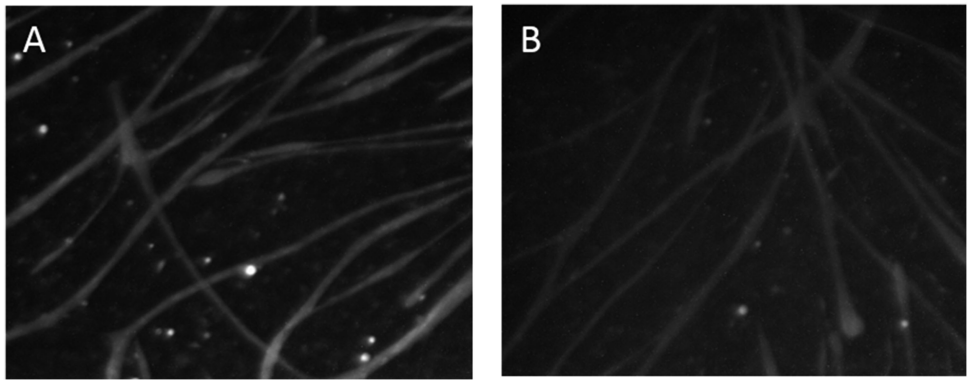

Fig. 6. Fluorescence images from 5-day old skeletal muscle cells stained with Fura-2 AM upon excitation at 385 nm (A) and 340 nm (B) using an upright microscope with a 10 x N.A 0.4 objective.

3.3 Spontaneously Triggered Ca^{2+} Transients

It is well established that the mammalian myotubes grown in culture exhibit spontaneous or induced action potentials with accompanying contractions [29]–[31]. On the sixth day of culture, the prepared myotubes started to contract spontaneously. These contractions are not simultaneously ubiquitous in the studied cell. The rhythmic contractions are visually discernible for several seconds. Once a contracting cell region is located in the petri dish, the samples are then illuminated with the 340/385 nm LEDs consecutively and the resulting fluorescence signal is recorded as a video for 100 s. A clear enhancement in the fluorescence intensity upon 340 nm excitation was observed in response to the cell contraction (no data is presented). The amounts of cytosolic free Ca^{2+} elevation as a result of the spontaneous contractions are calculated using the Eq. (1) from the fluorescence intensity ratio, R. The resulting spontaneous transients in the intracellular free Ca^{2+} concentration are presented in Fig. 7. The average increase in the spontaneously triggered Ca^{2+} concentration from the resting level is found to be 168 $\pm$ 11 nm. As seen in Fig. 7, both transients show approximate exponential decay. The decays are fitted with a single exponential approximation, and yield a time constant of 23 and 25 s respectively for panel A and B.

4. Discussion

This study took the advantages of the newly built high stability 340 nm LED by Prizmatix Ltd., Israel, to construct a fast switchable 340/385 nm LED excitation light source and showed that the

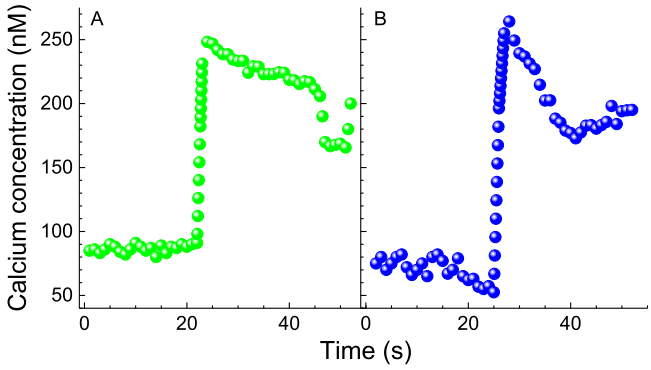

Fig. 7. (A–B): The calculated Ca^{2+} concentration in two different 6-day old skeletal muscle cells in response to the intermittent spontaneous contractions. The calculation has been done according to Eq. (1). The necessary parameters for the calculations are obtained from the calibration measurements.

assembled system as an alternative to conventional arc lamp source for Fura-2 based ratio-metric fluorescence microscopy imaging. The emission spectra of the 340/385 nm LED illumination system precisely matches the excitation spectra of the Fura-2 either in Ca^{2+} free or bound states. The newly constructed system can achieve a temporal resolution as short as 1 ms and can acquire the images at a rate as high as 1 kHz. The new light source has been employed in Fura-2 ratio-metric calcium imaging of live skeletal muscle cells. A similar work has been recently reported on the Fura-2 ratio-metric Ca^{2+} imaging in live tsA-201 cells and cultured hippocampal neurons [32].

The measured resting Ca^{2+} levels obtained in this study, 88 $\pm$ 3 nm, is in good agreement with the previously reported resting Ca^{2+} levels found in rat myotubes, 82 $\pm$ 6 [28], 80 nm found in pig skeletal muscles [33] and 100 nm measured in human skeletal muscles [34]. All the previous measurements were carried out using mercury arc lamp as the excitation source. The consistency of the present result with the earlier reports ensures that the newly constructed 340/385 nm LED illumination system as a reliable substitute for the arc lamp in UV ratio-metric imaging.

The new 340/385 nm LED illumination system has been further used in evaluating the transients of intracellular concentration of free Ca^{2+} ions in response to spontaneous contraction of the 6-day old rat myotubes. The average calcium elevation in the spontaneously elicited Ca^{2+} concentration from the resting level was found to be 163 $\pm$ 13 nm, which is comparable to the spontaneously triggered Ca^{2+} concentration increment in different types of cells [28], [35]. The Ca^{2+} transient in the presently measured rat myotubes lasted several seconds. Depending on the cell triggering, i.e., either spontaneously or by external stimulation, the reported Ca^{2+} transient decay times vary from hundreds of milliseconds to several minutes [21], [28], [35]–[38]. The fast switching capability of the constructed light source allows measuring the Ca^{2+} transient as fast as several milliseconds, which can provide much more temporal details than currently available ratio-metric Ca^{2+} imaging methods [39], [40].

5. Conclusion

In this report, we show that the newly constructed 340/385 nm LED excitation light source is a reliable and efficient alternative to an ordinary arc lamp source in Fura-2 based ratio-metric fluorescence microscopy imaging. The new illumination system precisely matches the excitation spectra of Fura-2 either in Ca^{2+} free or bound state. The newly built excitation source has been successfully applied in measuring spontaneous transients in the intracellular free Ca^{2+} concentration in rat myotubes. A new dual-LED fluorescence Spectra-Viewer is developed, which helps the user to simulate the ratio-metric Ca^{2+} imaging system online before the experiments. Alongside the advantages of the LEDs, the consistency of the present results with the previous reports, the new 340/385 nm LED illuminator system ensures its potential as a preferred light source for Fura-2 ratio-metric calcium imaging over existing light sources.

References

[1] T. Wallimann, *Calcium in Muscle Activation: A Comparative Approach by Johann Caspar Rüegg*, vol. 11. Berlin, Germany: Springer-Verlag, 1988, pp. 181–182.
[2] D. E. Clapham, "Calcium signaling," *Cell*, vol. 80, no. 2, pp. 259–268, 1995.
[3] M. J. Berridge, "Inositol trisphosphate and calcium signalling," *Nature*, vol. 361, pp. 315–325, 1993.
[4] M. J. Berridge, "Calcium microdomains: Organization and function," *Cell Calcium*, vol. 40, no. 5, pp. 405–412, 2006.
[5] M. D. Bootman, P. Lipp, and M. J. Berridge, "The organisation and functions of local Ca^{2+} signals," *J. Cell Sci.*, vol. 114, no. 12, pp. 2213–2222, 2001.
[6] P. A. Diliberto, X. F. Wang, and B. Herman, "Confocal imaging of Ca^{2+} in cells," in *A Practical Guide to the Study of Calcium in Living Cells (ser. Methods in Cell Biology)*, R. Nuccitelli, Ed. San Francisco, CA, USA: Academic, 1994, pp. 243–262.
[7] G. E. Stutzmann, F. M. LaFerla, and I. Parker, "Ca^{2+} signaling in mouse cortical neurons studied by two-photon imaging and photoreleased inositol triphosphate," *J. Neurosci.*, vol. 23, no. 3, pp. 758–765, 2003.
[8] J. R. Lakowicz *et al.*, "Fluorescence lifetime imaging of calcium using Quin-2," *Cell Calcium*, vol. 13, no. 3, pp. 131–147, 1992.
[9] K. Suzuki *et al.*, "Design and synthesis of calcium and magnesium ionophores based on double-armed diazacrown ether compounds and their application to an ion sensing component for an ion-selective electrode," *Anal. Chem.*, vol. 67, no. 2, p. 324–334, 1995.
[10] A. Marty, "Ca-dependent K channels with large unitary conductance in chromaffin cell membranes," *Nature*, vol. 291, pp. 497–500, 1981.
[11] E. S. Pierson *et al.*, "Tip-localized calcium entry fluctuates during pollen tube growth," *Develop. Biol.*, vol. 174, no. 1, pp. 160–173, 1996.
[12] A. K. Mudraboyina, L. Blockstein, C. C. Luk, N. I. Syed, and O. Yadid-Pecht, "A novel lensless miniature contact imaging system for monitoring calcium changes in live neurons," *IEEE Photon. J.*, vol. 6, no. 1, Feb. 2014, Art. no. 3900115.
[13] M. D. Bootman *et al.*, "Ca^{2+}-sensitive fluorescent dyes and intracellular Ca^{2+} imaging," *Cold Spring Harbor Protocols*, vol. 2013, pp. 83–89, 2013.
[14] D. Fixler *et al.*, "Differential aspects in ratio measurements of $[Ca^{2+}]i$ relaxation in cardiomyocyte contraction following various drug treatments," *Cell Calcium*, vol. 31, no. 6, pp. 279–287, 2002.
[15] D. Fixler *et al.*, "Cytoplasmic changes in cardiac cells during a contraction cycle detected by fluorescence polarization," *J. Fluorescence*, vol. 11, no. 2, pp. 89–100, 2001.
[16] G. Grynkiewicz, M. Poenie, and R. Y. Tsien, "A new generation of Ca^{2+} indicators with greatly improved fluorescence properties," *J. Biol. Chem.*, vol. 260, no. 6, pp. 3440–3450, 1985.
[17] D. A. Williams *et al.*, "Calcium gradients in single smooth muscle cells revealed by the digital imaging microscope using Fura-2," *Nature*, vol. 318, pp. 558–561, 1985.
[18] R. Y. Tsien, "Fluorescence measurement and photochemical manipulation of cytosolic free calcium," *Trends Neurosci.*, vol. 11, no. 10, pp. 419–424, 1988.
[19] D. Lipscombe *et al.*, "Imaging of cytosolic Ca^{2+} transients arising from Ca^{2+} stores and Ca^{2+} channels in sympathetic neurons," *Neuron*, vol. 1, no. 5, p. 355–365, 1988.
[20] A. Cornell-Bell *et al.*, "Glutamate induces calcium waves in cultured astrocytes: Long-range glial signaling," *Science*, vol. 247, no. 4941, pp. 470–473, 1990.
[21] J. Lainé *et al.*, "Development of the excitation-contraction coupling machinery and its relation to myofibrillogenesis in human iPSC-derived skeletal myocytes," *Skeletal Muscle*, vol. 8, pp. 1–13, 2018.
[22] R. M. Paredes *et al.*, "Chemical calcium indicators," *Methods*, vol. 46, no. 3, pp. 143–151, 2008.
[23] A. Shainberg, G. Yagil, and D. Yaffe, "Alterations of enzymatic activities during muscle differentiation in vitro," *Develop. Biol.*, vol. 25, no. 1, pp. 1–29, 1971.
[24] D. Adler *et al.*, "Weak electromagnetic fields alter Ca^{2+} handling and protect against hypoxia-mediated damage in primary newborn rat myotube cultures," *Pflügers Archiv, Eur. J. Physiol.*, vol. 468, no. 8, pp. 1459–1465, 2016.
[25] G. Skoglund *et al.*, "Physiological and ultrastructural features of human induced pluripotent and embryonic stem cell-derived skeletal myocytes in vitro," *Proc. Nat. Acad. Sci. USA*, vol. 111, no. 22, pp. 8275–8280, 2014.
[26] L. Turgeman and D. Fixler, "Photon efficiency optimization in time-correlated single photon counting technique for fluorescence lifetime imaging systems," *IEEE Trans. Biomed. Eng.*, vol. 60, no. 6, pp. 1571–1579, Jun. 2013.
[27] S. K. Kong and C. Y. Lee, "The use of fura 2 for measurement of free calcium concentration," *Biochem. Educ.*, vol. 23, no. 2, pp. 97–98, 1995.
[28] M. Grouselle *et al.*, "Fura-2 imaging of spontaneous and electrically induced oscillations of intracellular free Ca2+ in rat myotubes," *Pflügers Archiv*, vol. 418, no. 1, pp. 40–50, 1991.
[29] J. N. Barrett, E. F. Barrett, and L. B. Dribin, "Calcium-dependent slow potassium conductance in rat skeletal myotubes," *Develop. Biol.*, vol. 82, no. 2, pp. 258–266, 1981.
[30] J. A. Powell and D. M. Fambrough, "Electrical properties of normal and dysgenib mouse skeletal muscle in culture," *J. Cellular Physiol.*, vol. 82, no. 1, pp. 21–38, 1973.
[31] H. Schmid-Antomarchi *et al.*, "The all-or-none role of innervation in expression of apamin receptor and of apamin-sensitive Ca^{2+}-activated K+ channel in mammalian skeletal muscle," *Proc. Nat. Acad. Sci. USA*, vol. 82, no. 7, pp. 2188–2191, 1985.
[32] P. W. Tinning *et al.*, "A 340/380 nm light-emitting diode illuminator for Fura-2 AM ratiometric Ca^{2+} imaging of live cells with better than 5 nm precision," *J. Micros.*, vol. 269, no. 3, pp. 212–220, 2018.
[33] P. A. Iaizzo, W. Klein, and F. Lehmann-Horn, "Fura-2 detected myoplasmic calcium and its correlation with contracture force in skeletal muscle from normal and malignant hyperthermia susceptible pigs," *Pflügers Archiv*, vol. 411, no. 6, pp. 648–653, 1988.

[34] P. A. Iaizzo *et al.*, "The use of Fura-2 to estimate myoplasmic [Ca^{2+}] in human skeletal muscle," *Cell Calcium*, vol. 10, no. 3, pp. 151–158, 1989.
[35] K. Nobe *et al.*, "Preferential role of intracellular Ca(2+) stores in regulation of isometric force in NIH 3T3 fibroblast fibres," *J. Physiol.*, vol. 529, no. Pt 3, pp. 669–679, 2000.
[36] V. Eisner *et al.*, "Mitochondria fine-tune the slow Ca^{2+} transients induced by electrical stimulation of skeletal myotubes," *Cell Calcium*, vol. 48, no. 6, pp. 358–370, 2010.
[37] M. Casas *et al.*, "IP_3-dependent, post-tetanic calcium transients induced by electrostimulation of adult skeletal muscle fibers," *J. Gener. Physiol.*, vol. 136, no. 4, pp. 455–467, 2010.
[38] J. M. Eltit *et al.*, "Slow calcium signals after tetanic electrical stimulation in skeletal myotubes," *Biophys. J.*, vol. 86, no. 5, pp. 3042–3051, 2004.
[39] D. Fixler, Y. Namer, Y. Yishay, and M. Deutsch, "Influence of fluorescence anisotropy on fluorescence intensity and lifetime measurement: Theory, simulations and experiments," *IEEE Trans. Biomed. Eng.*, vol. 53, no. 6, pp. 1141–1152, Jun. 2006.
[40] O. Betzer *et al.*, "Theranostic approach for cancer treatment: Multifunctional gold nanorods for optical imaging and photothermal therapy," *J. Nanomater.*, vol. 16, no. 1, 2015, Art. no. 381.